Max-Planck-Institut
für Mathematik
in den Naturwissenschaften
Leipzig

Coarsening Dynamics for the Convective Cahn-Hilliard Equation

by

Stephen J. Watson, Felix Otto, Boris Y. Rubinstein, and Stephen H. Davis

Preprint no.: 35 2002

Coarsening Dynamics for the Convective Cahn-Hilliard Equation

Stephen J. Watson[1*†], Felix Otto[2], Boris Y. Rubinstein[1], Stephen H. Davis[1]

Engineering Sciences and Applied Mathematics, Northwestern University[1]
Institut für Angewandte Mathematik, Universität Bonn[2]

April 9, 2002

Abstract

We characterize the coarsening dynamics associated with a convective Cahn-Hilliard equation in one space dimension. First, we derive a sharp-interface theory based on a quasi-static matched asymptotic analysis. Two distinct types of discontinuity (kink and anti-kink) arise due to the presence of convection, and their motions are governed to leading order by a nearest-neighbors interaction dynamical system. Numerical simulations of the kink/anti-kink dynamics display marked self-similarity in the coarsening process, and reveal a *pinching* mechanism, identified through a linear stability analysis, as the dominant coarsening event. A self-similar period-doubling pinching ansatz is proposed for the coarsening process, and an analytical coarsening law, valid over all length scales, is derived. Our theoretical predictions are in good agreement with numerical simulations that have been performed both on the sharp-interface model and the original PDE.

1 Introduction

The Cahn-Hilliard equation governs the *spinodal decomposition* of binary alloys under isothermal conditions [1]. Here, an initially spatially homogeneous high-temperature mixture is driven to segregate by a uniform reduction in temperature (*quenching*). A fine-grained phase mixture is initially formed, and this morphology subsequently coarsens into larger-scale structures with a characteristic length scale $L(t)$. The Cahn-Hilliard theory utilizes an order parameter (phase fraction) with an associated double-well bulk (Helmhotz) free energy to describe this process. Among the properties of the CH theory [2] are the

*Corresponding author: watson@esam.nwu.edu
†On leave from Louisiana State University

phase selection rule for the mixture through a bi-tangent construction on the free energy, and the logarithmically slow coarsening rate in one space dimenison [3]:

$$\mathcal{L}(t) \sim \ln t.$$

The process of *thermal facetting*, in which a planar crystalline surface breaks up into hill (anti-kink) and valley (kink) structures following a change in temperature, is analogous to spinodal decomposition. The facetting transition in which a crystal surface is allowed to anneal in equilibrium with its vapor (or in vacuum), has also been modeled with equations of CH type [5, 6], in which the orientation of the local tangent plane serves as a (vector) order parameter and the surface tension induces an effective free energy. Here, the surface tension is sufficiently anisotropic that certain crystal surfaces are thermodynamically unstable and hence missing in the crystal equilibrium state (Wulff shape [7]). Stable facets correspond to bi-tangent points of the surface free energy, and the hill-valley structures coarsen with a rate depending on the mechanism of facet growth as well as the effective dimensions of the structure [8].

If the evolution of a crystal morphology possesses *growth* of some kind, then convective terms augment the CH structure [8, 9, 10]. Provided the strength of convection is small enough, spinodal decomposition reminiscent of CH again arises. However, because the convective term breaks the mirror symmetry $x \to -x$, several distinctions arise. In particular, the bi-tangent contruction for stable phases is destroyed, and kinks and anti-kinks are no longer symmetrically related [11]; this reflects the non-equilibrium nature of the growth process. This in turn results in enhanced coarsening rates relative to the CH theory. We remark that for sufficiently large convection the solutions do not coarsen in time but rather preserve fine-scale spatial oscillations. A study of this transition from coarsening to *kinetic roughening*, which is associated to the spatio-temporal chaos of the Kuramoto-Sivashinsky equation, has been carried out in [12].

A convective Cahn-Hilliard equation has been derived for the growth of thermodynamically unstable crystal surface into a hypercooled melt [10]. Here the crystal growth is controlled by attachment kinetics, which provides an additional flux of the order parameter, and emerges as a Burgers-type convection term. Convective - or driven - Cahn-Hilliard equations have also appeared as models for quenching of a homogeneous high temperature binary alloys in an external field [13], and unstable epitaxial growth with desorption [14].

In this paper we study the coarsening dynamics of a convective Cahn-Hilliard equation in one space dimension. In dimensionless form

$$q_t - qq_x = \left(q^3 - q - \epsilon^2 q_{xx}\right)_{xx}, \tag{1.1}$$

where the small parameter ϵ sets a length scale for transitions in x from negative to positive values of q (kink) or vice-versa (anti-kink). This equation has been derived as a model for kinetically controlled growth of two dimensional crystals

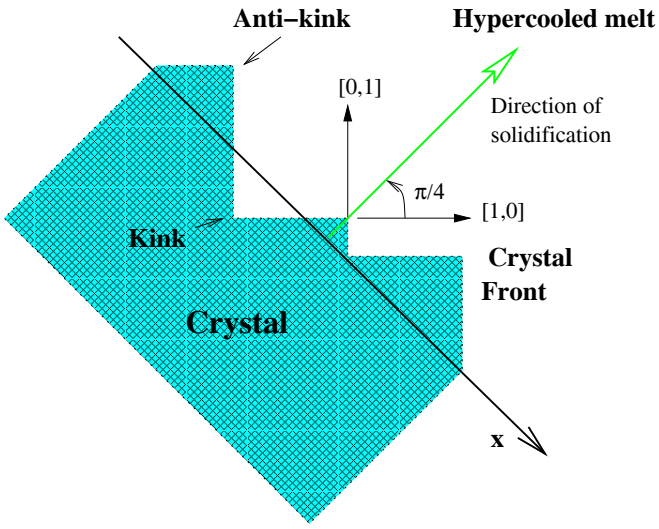

Figure 1: Schematic representation of a facetted 2-D crystal growing into its melt with a direction of solidification at $\pi/4$ to the principal crystallographic directions $[1, 0]$ and $[0, 1]$.

[10], and subsequently generalised in [15] following a geometric model proposed in [9]. In this setting q denotes the slope of the crystal surface; see Figure 1.

We perform a matched asymptotic analysis as $\epsilon \to 0^+$, that leads to a sharp interface theory of kink/anti-kink interaction valid over all non-dimensional length scales $L \gg \epsilon$. The convection-induced asymmetry between kink and anti-kink induces a convection-diffusion flux between neighbors, which in turn drives these discontinuities in a manner given by the Rankine-Hugoniot relation; recall that q is a conserved quantity. Through order $O(\epsilon)$ this results in a nearest neighbor interaction between kinks and anti-kinks. The resulting dynamical system generalizes the theory of Emmot and Bray [13], which is valid only for dimensionless length scales $\epsilon \ll L \ll 1$, to all length scales.

The dynamical system coarsens in time through the coalescence of kinks and anti-kinks. Numerical simulations reveal a marked self-similarity in the *coarsening path*, and also pinpoint the initially surprising prevalence of a particular ternary coalesence event. This *pinching* event involves the coalesence of two kinks with an anti-kink which results in a single kink remaining. A linear stability analysis of an initially periodic array of kink/anti-kinks confirms the observation by identifying a dominant instability which, when followed in to the nonlinear regime, displays such pinching.

We propose a self-similar period-doubling ansatz as a description of the coarsening process. It involves an initial disturbance of a spatially periodic array of kink/anti-kinks in the direction of the dominant linear-instability eigenvector by a scale invariant magnitude. This disturbance captures both the dominant

instability and the statistical deviations of the system. The resulting solution subsequently pinches in an explicitly calculable time, yielding a periodic array of twice the initial period. Motivated by the numerically observed self-similarity of the coarsening path, we iterate the above construction yielding our ansatz. A theoretical coarsening law for the mean length as a function of time, which is valid over all length scales, then follows from the ansatz. When we restrict our analysis to $L \ll 1$ we recover the scaling law

$$\mathcal{L}(t) \sim ct^{1/2},$$

previously deduced by Emmot and Bray [13]. However, since we also describe the coarsening path, we are also able to identify the scaling constant c. In addition, our results agree with the numerically computed coarsening rates of Golovin et. al. [12], which apply to length scales $\epsilon << \mathcal{L} < \infty$.

2 The statement of the problem

We consider the following one-dimensional *convective Cahn-Hilliard* equation:

$$q_{\bar{t}} - Vqq_{\bar{x}} = \mu\left(q^3 - q - \gamma^2 q_{\bar{x}\bar{x}}\right)_{\bar{x}\bar{x}} \tag{2.1}$$

where the dimensionless order parameter $q(\bar{x}, \bar{t})$ is a function of space $\bar{x} \in \mathbb{R}$ and time $\bar{t}$, V is a speed ($[V] = LT^{-1}$), μ is a mobility ($[\mu] = L^2T^{-1}$) and γ is a microscopic length scale ($[\gamma] = L$). Equation (2.1) serves, for example, as a phenomenological model of facetting in kinetically controlled crystal growth [10].

The convection coupled to diffusion supplies the *Peclet* length scale $l_{\mathcal{P}}$ given by

$$l_{\mathcal{P}} = \frac{\mu}{V},$$

We now re-scale (2.1) with respect to the length scale $l_{\mathcal{P}}$ and time scale $t_{\mathcal{P}} = \frac{\mu}{V^2}$. Setting

$$x = \frac{\bar{x}}{l_{\mathcal{P}}}, \quad \text{and} \quad t = \frac{\bar{t}}{t_{\mathcal{P}}},$$

we arrive at the dimensionless form

$$q_t - qq_x = \left(q^3 - q - \epsilon^2 q_{xx}\right)_{xx}, \tag{2.2}$$

where

$$\epsilon = \frac{\gamma}{l_{\mathcal{P}}}.$$

Now when $\epsilon \sim 1$, the morphologies of solutions do not coarsen in time but rather remain *rough* [12]. This is related to the fact that formally the convective Cahn-Hilliard approaches the Kuramoto-Sivashinsky (KS) equation as $\epsilon \to \infty$, and solutions of the (KS) eqauation are known to display spatio-temporal chaos.

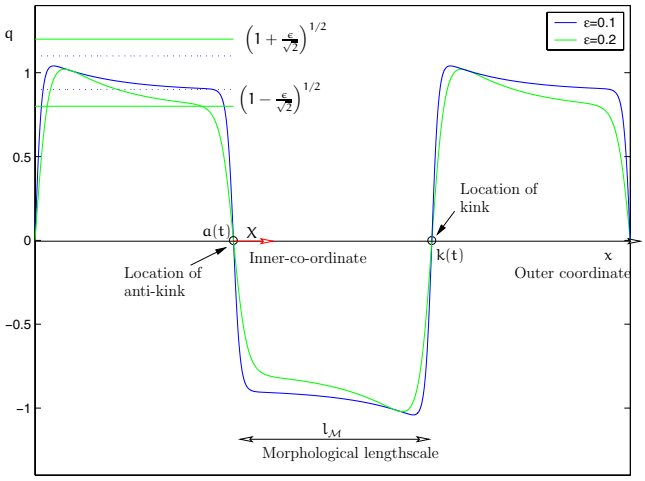

Figure 2: A representative sequence of kinks and anti-kinks

We consider the regime of disparate length scales

$$\epsilon = \frac{\gamma}{l_{\mathcal{P}}} \ll 1.$$

Here the spatially homogeneous state $q = 0$ is unstable and upon disturbance develops a periodic structure of alternating *kinks* and *anti-kinks* with wavelength $\lambda \sim \gamma$, as determined from a linear stability analysis (see Fig. 2).

The solution subsequently coarsens in time with a morphology that has a characteristic length scale, $l_{\mathcal{M}}$ (the *morphological length scale*). Three natural regimes arise in this process and have been previously analysed numerically [12, 13]:

$$\gamma \ll l_{\mathcal{M}} \ll l_{\mathcal{P}} \qquad \text{Power law} \qquad \text{(P)}$$
$$\gamma \ll l_{\mathcal{M}} \simeq l_{\mathcal{P}} \qquad \text{Intermediate regime} \qquad \text{(I)}$$
$$\gamma \ll l_{\mathcal{P}} \ll l_{\mathcal{M}} \qquad \text{Logarithmically slow} \qquad \text{(L)}$$

The details of the morphological evolution in the intermediate regime is particularly interesting because of the unexpected persistence of the preceding power law behavior that is observed [12].

3 Sharp interface theory

The governing equation (2.2) is singularly perturbed in the limit $\epsilon \to 0^+$. In this section we perform the associated matched asymptotic expansions. Since the parameter ϵ sets a length scale for transitions, we shall see that the associated outer problem yields a sharp-interface theory.

3.1 Asymptotic analysis for $\gamma \ll l_P$

We refer to (2.2) as the outer equation, since $\epsilon \to 0^+$ yields a singular perturbation. The inner equation arises from re-scaling to the inner length scale ϵ (in units of l_P). Since the kinks and anti-kinks are in general moving, we need to select an inner co-ordinate with respect to a moving frame. So, for the kink at $x = k(t;\epsilon)$, we take the inner-coordinate X to be

$$X = \frac{x - k(t;\epsilon)}{\epsilon},$$

and re-write (2.2) in terms of the inner solution $Q(X,t) = q(x,t)$ as

$$\epsilon^2 Q_t - \epsilon \dot{k} Q_X - \epsilon Q Q_X = \left(Q^3 - Q - Q_{XX}\right)_{XX} \ ; \tag{3.1}$$

similarly for the anti-kink $a(t)$.

Remark 1 *We give a complete matched asymptotic analysis through order* $O(\epsilon)$ *in the Appendix. Therein, we establish that the kink velocity* $\dot{k}(t)$ *(with respect to the Peclet length scale) is of order* $O(\epsilon)$ *since* $\epsilon = 0$ *corresponds to a stationary solution.*

Since the kink and anti-kink velocities are of order $O(\epsilon)$ (see Appendix) it follows that (3.1) is asymptotically equivalent through order $O(\epsilon)$ with the time-independent equation

$$-\epsilon Q Q_X = \left(Q^3 - Q - Q_{XX}\right)_{XX}. \tag{3.2}$$

Now (3.2) has two exact solutions $\mathcal{K}(X)$ and $\mathcal{A}(X)$, identified in [11], given by

$$\mathcal{K}(X) := \left(1 + \frac{\epsilon}{\sqrt{2}}\right)^{1/2} \tanh\left[\left(1 + \frac{\epsilon}{\sqrt{2}}\right)^{1/2} X\right] \qquad \text{(Kink)} \tag{3.3}$$

and

$$\mathcal{A}(X) := -\left(1 - \frac{\epsilon}{\sqrt{2}}\right)^{1/2} \tanh\left[\left(1 - \frac{\epsilon}{\sqrt{2}}\right)^{1/2} X\right], \qquad \text{(Anti-Kink)} \tag{3.4}$$

which will be matched to the outer solutions.

Remark 2 *There is a family of stationary profiles associated with the transition from positive to negative values of* q *[13], while the anti-kink profile is the unique profile connecting negative to positive values of* q*. Our choice of kink leads to a Dirichlet outer problem.*

We note here that the asymptotic values as $X \to \infty$ of $\mathcal{K}(X)$ and $\mathcal{A}(X)$ are

$$\lim_{X \to \pm\infty} \mathcal{K}(X) = \pm\left(1 + \frac{\epsilon}{\sqrt{2}}\right)^{1/2},$$
$$\lim_{X \to \pm\infty} \mathcal{A}(X) = \mp\left(1 - \frac{\epsilon}{\sqrt{2}}\right)^{1/2}.$$

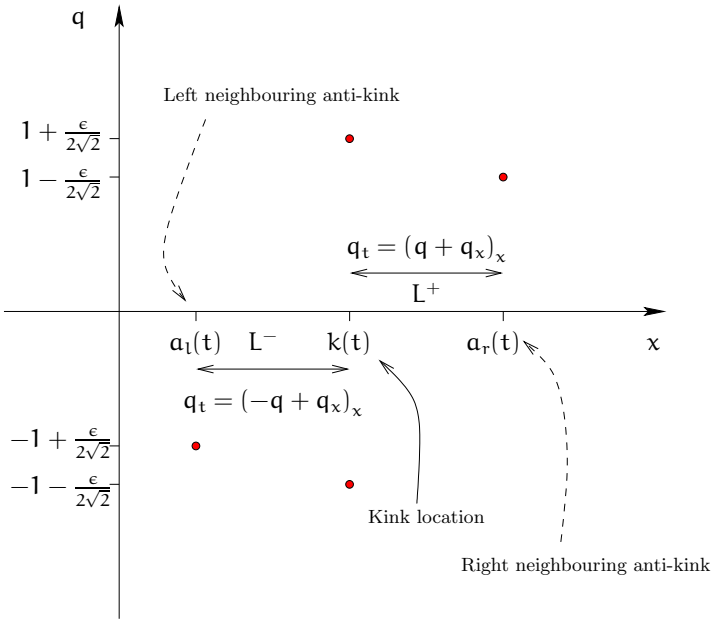

Figure 3: The $0(\epsilon)$ sharp interface limit

We see that the presence of convection ($\epsilon \neq 0$) introduces a fundamental asymmetry between kinks and anti-kinks, which is not present in the CH theory ($\epsilon = 0$). On a deeper level, this asymmetry is a reflection of the non-equilibrium nature of the underlying phase-transformation process when convection is present.

We now match these inner solutions to the outer solution, which we represent in the form

$$q(x,t) = q_0(x,t) + q_1(x,t)\epsilon + O(\epsilon^2).$$

It follows from the matched asymptotic analysis presented in the Appendix that the combined approximation $q^c := q_0 + q_1\epsilon$ is equivalent through order $0(\epsilon)$ with the conservation law

$$q^c{}_t + J_x = 0 \quad \text{for} \quad (x,t) \in \mathbb{R} \times [0,\infty), \tag{3.5}$$

with flux J given by

$$J = \begin{cases} -q^c - q^c{}_x & x \in (\, k(t), a(t)\,) \\ \\ q^c - q^c{}_x & x \in (\, a(t), k(t)\,) \end{cases}, \tag{3.6}$$

and subject to the Dirichlet boundary conditions

$$\begin{aligned} q^c(k(t)^-) &= -1 - \tfrac{1}{2\sqrt{2}}\epsilon \qquad q^c(k(t)^+) = 1 + \tfrac{1}{2\sqrt{2}}\epsilon \\ q^c(a(t)^-) &= 1 - \tfrac{1}{2\sqrt{2}}\epsilon \qquad q^c(a(t)^+) = -1 + \tfrac{1}{2\sqrt{2}}\epsilon \ , \end{aligned} \tag{3.7}$$

where $q^c(k(t)^-)$ and $q^c(k(t)^+)$ denote the limiting value of q^c as the kink location $k(t)$ is approached from the left and the right respectively; similarly for the anti-kinks; see Figure 3.

It follows from the conservation law (3.5) that the speed of the kink $\dot{k}(t)$ (k-shock) is given by the Rankine-Hugoniot relation

$$\dot{k}(t)[q]_{k(t)} = [J]_{k(t)}, \tag{R}$$

where $[J]_{k(t)}$ and $[q]_{k(t)}$ denote, respectively, the jump in the flux J and the order parameter q across the kink at $x = k(t)$; similarly for the anti-kink.

Since the kink and anti-kink velocities are order $O(\epsilon)$, it follows that (3.5) is equivelent through order $O(\epsilon)$ with the quasi-static condition

$$J_x = 0. \tag{3.8}$$

Utilizing the notation of Figure 3, the function q^c can now be computed from (3.6), (3.7) and (3.8) yielding

$$q^c(x) = \begin{cases} -1 - \frac{\varepsilon}{2\sqrt{2}} + \frac{\varepsilon}{\sqrt{2}} \frac{1 - e^{[x - a_l(t) - L^-]}}{1 - e^{-L^-}} & a_l(t) \le x \le k(t) \\ 1 + \frac{\varepsilon}{2\sqrt{2}} - \frac{\varepsilon}{\sqrt{2}} \frac{1 - e^{-[x - k(t)]}}{1 - e^{-L^+}} & k(t) \le x \le a_r(t) \end{cases} ; \tag{3.9}$$

The flux J between a kink and anti-kink now follows by direct calculation from (3.6) and appears as

$$J = \frac{\epsilon}{2\sqrt{2}} \frac{1}{e^{\mathcal{L}} - 1} \ , \tag{3.10}$$

where $\mathcal{L} = |k(t) - a(t)|$ is the distance between the neighbouring kink and anti-kinks.

The $O(\epsilon)$ composite solution, obtained from matching inner and outer solutions, is plotted in Figure 2 for a choice of parameters associated with the regime $\gamma \ll l_{\mathcal{M}} \simeq l_{\mathcal{P}}$. We note that the kink amplitude is suppressed while the anti-kink amplitude is barely affected. This circumstance is either enhanced or diminished by the respective increase or decrease of the separation between kink and anti-kink.

4 Kink-antikink dynamics

We have envisioned the solutions to (2.1) as an alternating sequence of kinks $\mathcal{K}[X - k(t)]$ and anti-kinks $\mathcal{A}[X - a(t)]$, which are matched through the outer variable x associated with the Peclet length scale l_P; the points $k(t)$ and $a(t)$ being the kink and anti-kink locations, respectively. We now present a study of the dynamical system associated with these locations.

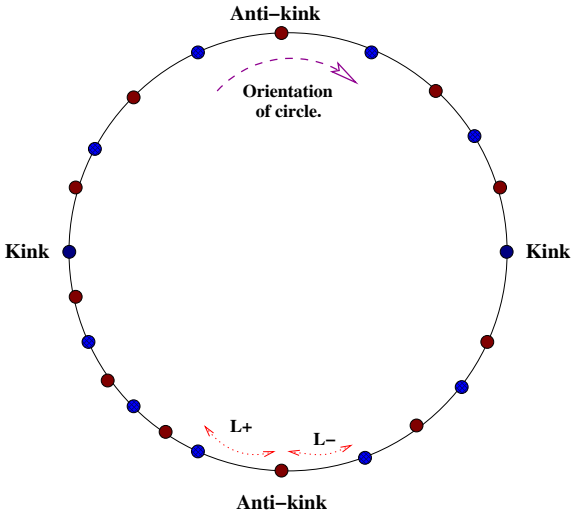

Figure 4: Kink and anti-kink dynamical system

4.1 The coarsening dynamical system

We consider an alternating sequence of kinks and anti-kinks placed on a domain, either the unbounded line or a circle of prescribed circumference The velocities of the kinks $\dot{k}(t)$ and anti-kinks $\dot{a}(t)$ through order $0(\varepsilon)$ follow from (R), (3.7) and (3.10) and satisfy

$$\dot{k}(t) = \tilde{\varepsilon}\left[\hat{f}\left(L^{+}\right) - \hat{f}\left(L^{-}\right)\right] \tag{4.1}$$

$$\dot{a}(t) = \tilde{\varepsilon}\left[\hat{f}\left(L^{-}\right) - \hat{f}\left(L^{+}\right)\right] \ , \tag{4.2}$$

where $\tilde{\varepsilon} = \varepsilon/4\sqrt{2}$,

$$\hat{f}(l) := \frac{1}{e^{l} - 1}, \tag{4.3}$$

and L^{+} and L^{-} denote the distance (arc-length) to the right and left neighbors of the kink or antikink; see Figure 4.

The outcome of encounters between kinks and anti-kinks is readily visualized via the facetted-crystal application. First, if a pair meet, they annihilate since the interpolating facet disappears. Now in the case of coalescence of higher order, e.g. the ternary collision, a *parity law* arises. Namely, even groupings annihilate, and odd groupings result in the appearance of the dominant type. So, for example, in the case of two kinks colliding with a single anti-kink, we obtain a kink. Through this process of annihilation the average length scale of the structure grows.

Remark 3 *The dynamical system is non-standard since the dimension of the system shrinks in time as particles annihilate. We coin the term* coarsening dynamical system *to denote such dimensional reducing systems.*

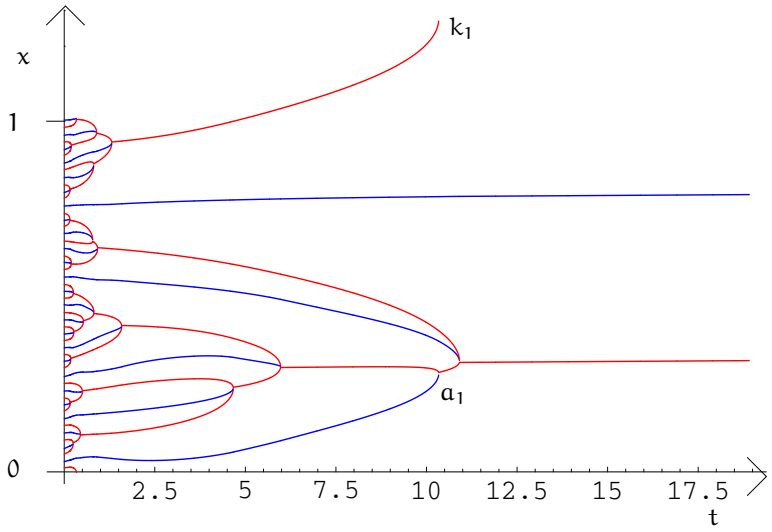

Figure 5: Numerical simulation of kink/anti-kink dynamics on a circle of circumference 1. The kink trajectories are marked in red and the anti-kink trajectories in blue. Note that the kink marked k_1 coalesces with the anti-kink marked a_1.

4.2 Simulations

A numerical code simulating the kink/anti-kink dynamics (4.1) and (4.2) has been written using Mathematica. We treated the problem of n kink/anti-kink pairs on a circle of prescribed circumference L (i.e. periodic boundary conditions on an interval of length L) for $\epsilon \ll 1$. For initial conditions we take an array of evenly spaced particles with separation $d := L/2n$ (see Figure 4), and then perturb each location by a random distance taken from a normal distribution centered at 0 with covariance $d/20$. Coalescence of particles is identified when the distance between two particles come within the prescribed tolerance, $\epsilon/10$.

We present in figure 5 the result of a numerical simulation for 25 kink/anti-kink pairs placed on a domain of unit length with $\epsilon = 0.005$. An initially surprising feature of the simulations is the prevalence of *pinching events*, whereby two kinks converge on an anti-kink resulting in an anti-kink. One can also note a marked degree of self-similarity during coarsening with pinching appearing as the major coalescence event The coarsening stops at the appearance of a single kink/anti-kink pair, which subsequently preserve a fixed separation.

4.3 Linear Stability Analysis

Here we perform a linear stability analysis of an alternating array of equally spaced kink/anti-kinks on a circle. We then deduce the stability for the line as

the limit of infinite circumference for the circle.

Let l_0 be the separation of an equi-spaced array of kink/antikinks on a circle of circumference $4nl_0$ ($n \in \mathbb{N}$). The linearization of the $4n$ dimensional dynamical system (4.1) and (4.2) about this state yields the $4n \times 4n$ matrix

$$A = -\hat{f}'(l_0) \begin{bmatrix} 2 & -1 & 0 & & & & ... & & & 0 & -1 \\ 1 & -2 & 1 & 0 & & & ... & & & & 0 \\ 0 & -1 & 2 & -1 & 0 & & ... & & & & 0 \\ 0 & & 1 & -2 & 1 & 0 & & & & & 0 \\ & & & & . & . & . & & & & \\ & & & & . & . & . & & & & \\ 0 & & & & & & ... & 0 & -1 & 2 & -1 \\ 1 & 0 & & & & & ... & & 0 & 1 & -2 \end{bmatrix}$$

whose eigenvalues determine the instability of the uniform state. Notice that the each successive row is a simple cyclic permutation of the previous row followed by multiplication by -1, and also, $-f'(l_0) > 0$.

We now present a characterization of the eigenvalues and eigenvectors of A. in terms of the complex 4n'th roots of unity:

$$r_j := e^{i(\frac{\pi}{2n})j} \qquad \text{where} \quad j = 0, 1, ..., 4n-1$$

First, for each $j = 0, 1, ...$, we define the k'th component of the vectors $\mathbf{u}^{(j)}, \mathbf{v}^{(j)} \in \mathbb{C}^{4n}$ as follows:

$$\mathbf{u}^{(j)}_k = (r_j)^k \ , \qquad \mathbf{v}^{(j)}_k = (-r_j)^k \qquad k = 1, ..., 4n.$$

We claim for each $j = 1, ..., 2n-1$, that the vectors $\mathbf{e}_j$, ω_j given by

$$\mathbf{e}_j := \left[1 + \cos\left(\frac{j\pi}{2n}\right)\right]^{1/2} \mathbf{u}_j + \left[1 - \cos\left(\frac{j\pi}{2n}\right)\right]^{1/2} \mathbf{v}_j,$$
$$\omega_j := \left[1 + \cos\left(\frac{j\pi}{2n}\right)\right]^{1/2} \mathbf{u}_j - \left[1 - \cos\left(\frac{j\pi}{2n}\right)\right]^{1/2} \mathbf{v}_j$$

are eigenvectors of A with associated eigenvalues

$$\lambda_j = 2\sin\left(\frac{j\pi}{2n}\right), \qquad \gamma_j = -2\sin\left(\frac{j\pi}{2n}\right) \ ,$$

respectively. This follows from a general theorem on alternating circulant matrices motivated by this work [16]. Furthermore, the vectors $\mathbf{u}_0, \mathbf{v}_0$ are generalised eigenvectors of A with eigenvalue 0, and the set of vectors

$$\{\mathbf{u}_0, \mathbf{v}_0, \mathbf{e}_1, ..., \mathbf{e}_{n-1}, \omega_1, ..., \omega_{n-1}\}$$

constitute a basis for $\mathbb{C}^{4n}$.

The largest eigenvalue of 2 is attained when $j = n$, and the associated eigenvector is the 4-periodic vector

$$\mathbf{e}_n = [1, 0, -1, 0, ...].$$

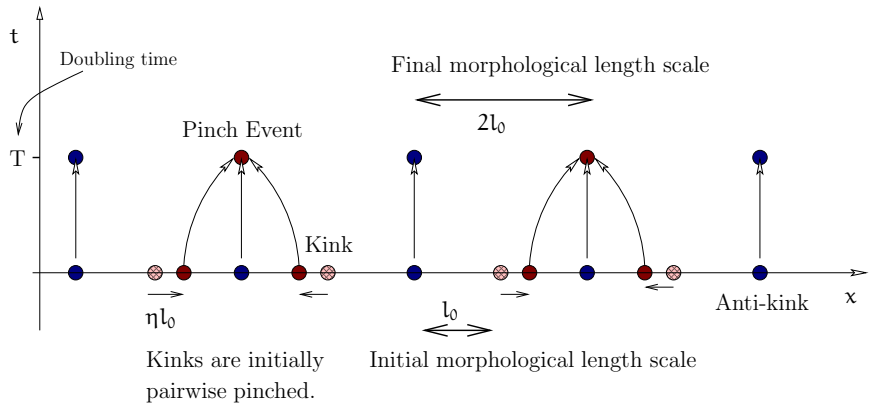

Figure 6: The period doubling ansatz

We note that in this most unstable direction the anti-kinks remain fixed and the kinks are "pinched" pairwise. Also, the structure of this unstable mode is independent π; i.e of the circumference of the circle. Hence, we conclude that this is the most unstable mode for the unbounded line as well.

5 Coarsening dynamics

We introduce here a *coarsening ansatz* for the sharp interface theory. It is based on several working hypotheses:

- The dominant mode of instability arises from the linearised problem.
- The coarsening solutions are self-similar; motivated by the numerical simulations.
- The statistical component of an evolution may be characterized through a scale-invariant disturbance used to initiate the coarsening.

Based on these ansatzen we deduce a theoretical coarsening law for the average length scale as a function of time. It stands in excellent agreement with results obtained from direct simulation of the model equations. A precise description follows.

5.1 The coarsening ansatz

An equally spaced array of kink/antikinks on a domain $\mathcal{I}$ (circle or line) is an unstable critical point for the dynamical system (4.1) and (4.2). Motivated by the linear stability analysis of Section 4.3, we study the initial-value problem associated with a scale-invariant disturbance of this state in the direction of the most unstable eigenvector. Specifically, we fix the location of the anti-kinks

while pairwise pinching the kinks together by a scale invariant distance ηl_0, where l_0 is the initial separation and $\eta > 0$ is a fixed small constant; see Figure 6.

It follows from the symmetry of the initial data that the solution is a periodic extension of the elementary initial-value problem involving two pairs of kinks and anti-kinks on a circle of circumference $4l_0$, subject to the dynamics given by (4.1) and (4.2) and the initial conditions illusrated in Figure 7. One sees that the anti-kinks will remain fixed as the solution evolves, while the two kinks move towards the initially closer anti-kink. They subsequently coalesce at the anti-kink, leaving a kink, in a finite time T characterized by the simple target-time problem:

$$\begin{aligned} \frac{ds}{dt} &= \tilde{\varepsilon}\left[\hat{f}(l_0 - s) - \hat{f}(l_0 + s)\right] \\ s(0) &= \eta l_0 \\ s(T^-) &= l_0, \end{aligned}$$

Applied to Figure 6 we see that the an initial morphological length scale l_0 will be doubled in the *doubling time* T.

We may explicitly calculate T as a function of the initial length l_0, and η:

$$\begin{aligned} T = \hat{T}(l_0, \eta) &= \frac{1}{\tilde{\varepsilon}} \int_{\eta l_0}^{l_0} \frac{ds}{f(l_0 - s) - f(l_0 + s)} \\ &= \frac{1}{\tilde{\varepsilon}} \left(e^{l_0/2} + e^{-l_0/2}\right) \left[\operatorname{arctanh}\left(e^{-\frac{\eta l_0}{2}}\right) - \operatorname{arctanh}\left(e^{-\frac{l_0}{2}}\right)\right] \\ &\quad - \frac{1}{\tilde{\varepsilon}} \left(\ln\left[e^{\frac{1-\eta}{2} l_0}\right] + \ln\left[e^{l_0} - 1\right] - \ln\left[e^{l_0} - e^{l_0(1-\eta)}\right]\right). \end{aligned} \tag{5.1}$$

Remark 4 *We view the dimensionless parameter η as measuring the deviation of lengths in the coarsening structure from the mean length. Of course, this implicitly assumes that the distribution of lengths around the mean is scale-invariant throughout the coarsening. One may chose to go beyond self-similarity and assume a dependence of η on the length scale l.*

5.2 Theoretical coarsening law

Assuming self similarity in the coarsening process, we may iterate this period doubling ansatz. This yields a geometric increase in the length scale in a known time period. Idealizing the initial-length scale to be infinitesimally small relative to the observed length scales, we deduce the following (implicit) theoretical coarsening law for the morphological length scale $l_{\mathcal{M}}$ as a function of time t.

$$t = \sum_{i=1}^{i=\infty} \hat{T}\left(\frac{l_{\mathcal{M}}}{2^i}, \eta\right) \tag{5.2}$$

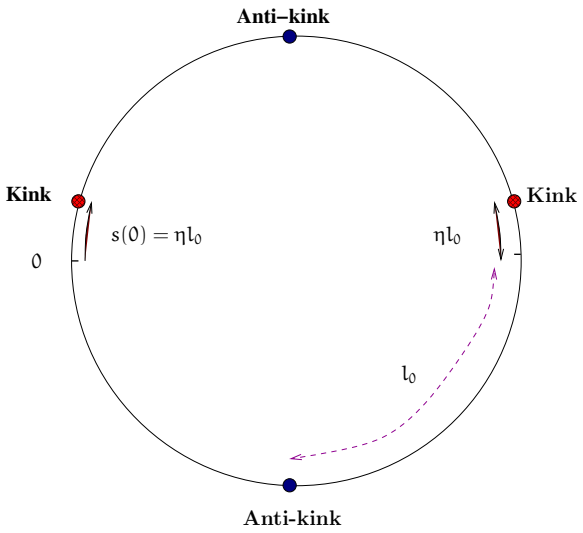

Figure 7: Elementary pinching event

A numerical plot of this theoretical scaling law is displayed in Figure 8 for $\tilde{\epsilon} = .001$ and $\eta = .001$. A numerical plot of the associated "infinitesimal scaling exponent" is shown in Figure 9. One notes the surprising persistence of the scaling $L(t) \sim t^{1/2}$ for $\epsilon \ll L \sim 0(1)$, followed by a transition to the exponentially slow regime as $L \to \infty$.

The scaling law $L(t) \sim t^{1/2}$, which arises in the the regime $L \ll 1$, may be understood by the following scaling arguement. First, there are two types of length intervals between kink and anti-kink, distinguished by whether a kink or anti-kink appears at the left end-point, and which we denote by L_k and L_a respectively. It follows from (4.1) and (4.2) that

$$\dot{L}_k(t) = \tilde{\epsilon}\left(\frac{1}{e^{L_a^-} - 1} - \frac{1}{e^{L_a^+} - 1}\right) \tag{5.3}$$

$$\dot{L}_a(t) = \tilde{\epsilon}\left(\frac{1}{e^{L_k^+} - 1} - \frac{1}{e^{L_k^-} - 1}\right) \tag{5.4}$$

where the superscripts $+$ and $-$ denote right and left neighboring intervals. Noting that

$$\frac{1}{e^L - 1} \sim \frac{1}{L} \qquad \text{as} \quad L \to 0^+ \ ,$$

the system (5.3) and (5.4) has the asymptotic form

$$\dot{L}_k(t) = \tilde{\epsilon}\left(\frac{1}{L_a^-} - \frac{1}{L_a^+}\right) \tag{5.5}$$

$$\dot{L}_a(t) = \tilde{\epsilon}\left(\frac{1}{L_k^+} - \frac{1}{L_k^-}\right) \tag{5.6}$$

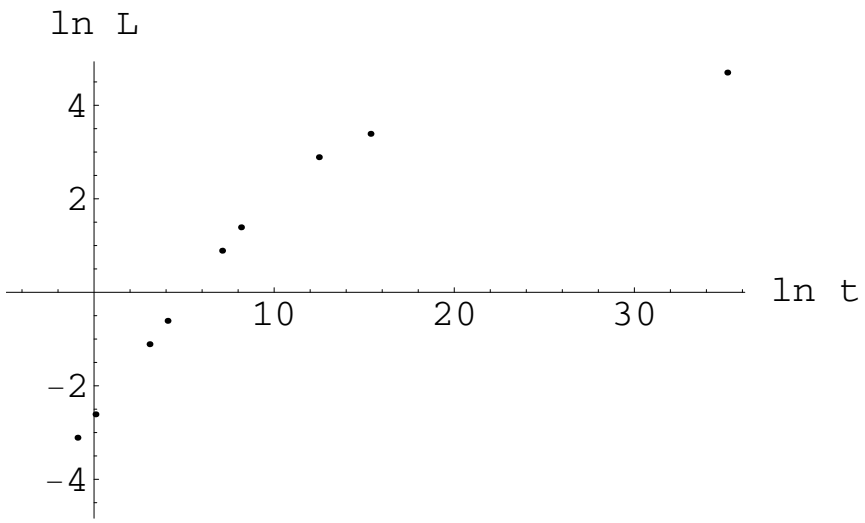

Figure 8: Numerical plot of the theoretical scaling law based on the period doubling ansatz.

as $L \to 0^+$. Now, (5.5) and (5.6) are invariant with respect to the scaling

$$t \to \lambda^2 t, \qquad l \to \lambda l. \tag{5.7}$$

Hence, if there exists a universal law for the growth of the a characteristic length scale $L(t)$ associated with the dynamical system (5.5) and (5.6), then

$$L(t) \sim t^{1/2}.$$

However, since we have specified a coarsening path, we are also able to identify the scaling constant from our theoretical formula as follows. First, the doubling time (5.1) has the asymptotic form

$$\hat{T}(l_{\mathcal{M}}, \eta) = \frac{1}{4}\left(\eta^2 - 2\ln\eta - 1\right) l_{\mathcal{M}}^2 \qquad \text{as} \qquad l_{\mathcal{M}} \to 0^+.$$

Hence, the theoretical scaling law (5.2) yields

$$l_{\mathcal{M}} = \frac{\sqrt{3}}{\eta^2 - 2\ln\eta - 1} t^{1/2} \qquad \text{as} \qquad l_{\mathcal{M}} \to 0^+.$$

Note that scaling constant $c(\eta) := \frac{\sqrt{3}}{\eta^2 - 2\ln\eta - 1}$ is monotone increasing in the interval $\eta \in (0, 1)$, and furthermore

$$\lim_{\eta \to 0^+} c(\eta) = 0 \qquad \text{and} \qquad \lim_{\eta \to 1^-} c(\eta) = \infty.$$

One may envision determining η from a numerical simulation of the full problem.

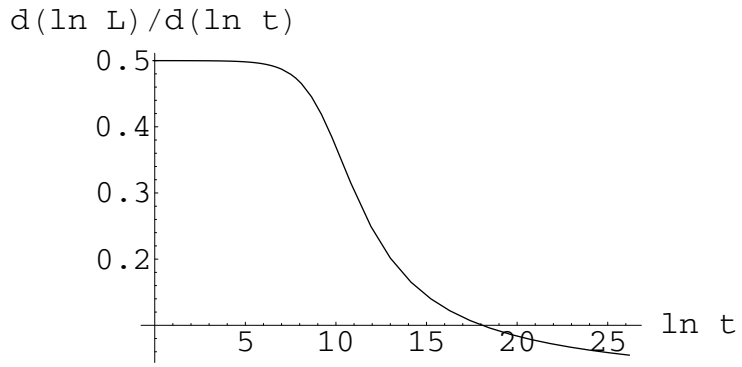

Figure 9: The "infinitesimal scaling exponent" based on the period doubling ansatz.

6 Conclusions

We have considered the coarsening dynamics of a two-phase convective Cahn-Hilliard equation. A sharp interface theory for the evolution of *phase boundaries* is derived through a matched asymptotic expansion arising when the phase boundary width $\epsilon \to 0^+$. To leading order the system is described by a nearest neighbour dynamical system which coarsens in time through the coalesence of phase boundaries. A pinching mechanism is identified through a linear stability analysis as the dominant coarsening event. This is confirmed by numerical simulations, which furthermore display a marked self-similarity in the coarsening path. A self-similar period doubling ansatz, involving a scale invariant recursion of the elementary pinching mechanism, is subsequently proposed as a description of the entire coarsening path. This yields, in turn, a theoretical coarsening law of the morphological length scale $l_{\mathcal{M}}$ as a function of time t which is in good qualitative agreement with both the direct computations of the coarsening dynamical system performed here, and also the numerical simulations of the convective Cahn-Hilliard equation [12].

The coarsening dynamical system approach developed here offers a flexible framework for the identification of coarsening laws in 1-D systems where localised structures (defects) interact. It embodies the principle that the evolution of structure is essentially determined by the local structure of the defects and there mutual interaction.

Acknowledgment. S.J.W. was supported by the Max-Planck-Institute for Mathematics in the Sciences (MIS), Leipzig in the initial stages of this project and later by the NSF N.I.R.T. grant # DMR-0102794. SHD was supported by

the NSF N.I.R.T. grant # DMR-0102794.

A Matched asymptotic analysis

The governing equation (2.2) is singularly perturbed in the limit $\epsilon \to 0^+$, and so is referred to as the outer equation. In this section we perform the associated matched asymptotic expansions. Since the parameter ϵ sets a length scale for transitions, we shall see that the associated outer problem yields a sharp-interface theory.

We assume the asymptotic expansion of (2.2) takes the form

$$\begin{aligned} q &= q_0(x) + q_1(x)\epsilon + ... && \text{(Outer expansion)} \\ k(t,\epsilon) &= k_0(t) + k_1(t)\epsilon + ... && \text{(Kink expansion)} \\ a(t,\epsilon) &= a_0(t) + a_1(t)\epsilon + ... && \text{(Anti-kink expansion)} \end{aligned}$$

The inner equation arises from re-scaling to the inner length scale ϵ (in units of l_p). Since the kinks $k(t;\epsilon)$ and anti-kinks $a(t;\epsilon)$ are in general moving, we need to select an inner co-ordinate with respect to a moving frame. So, for the kink at $x = k^i(t;\epsilon)$, we take the inner-coordinate X to be

$$X = \frac{x - k(t;\epsilon)}{\epsilon},$$

and re-write (2.2) in terms of the inner solution $Q(X,t) = q(x,t)$ as

$$\epsilon^2 Q_t - \epsilon \dot{k}(t;\epsilon) Q_X - \epsilon Q Q_X = \left(Q^3 - Q - Q_{XX}\right)_{XX} \ . \tag{A.1}$$

We proceed in a similar fashion for the anti-kink $a(t)$.

Now q satifies the conservation law

$$q_t + J_x = 0$$

where

$$J = -\hat{W}'(q)_x + \frac{\epsilon}{2} q^2 + \epsilon^2 q_{xxx}. \tag{A.2}$$

Hence, across the kinks and anti-kinks we have the Rankine-Hugoniot relation:

$$\dot{k}(t)[q]_{k(t;\epsilon)} = [J]_{k(t;\epsilon)}, \tag{R}$$

where $[J]_{k(t;\epsilon)}$ and $[q]_{k(t;\epsilon)}$ denote, respectively, the jump in the flux J and the order parameter q across the kink at $x = k(t;\epsilon)$; similarly for the anti-kink.

Before proceeding with the matching, we convert the free boundary-value problem associated with the outer solution to a fixed domain by introducing the following co-ordinate transformation. Assume that the initial distribution of kink and anti-kink locations is given by k^i, $a^i \in \mathbb{R}$ ($i \in \mathbb{Z}$) where

$$k^i < a^i < k^{i+1} \qquad \forall i \in \mathbb{Z}$$

We define $\Psi : \mathbb{R} \times [0, T) \times [0, \bar{\epsilon}) \to \mathbb{R}$, through

$$\Psi(y,t,\epsilon) := \begin{cases} k_i(t,\epsilon) + \frac{a_i(t,\epsilon)-k_i(t,\epsilon)}{a^i-k^i}(y-k^i) & x \in (k^i, a^i) \\ \\ a_{i-1}(t,\epsilon) + \frac{k_i(t,\epsilon)-a_{i-1}(t,\epsilon)}{k^i-a_{i-1}}(y-a_{i-1}) & x \in (a_{i-1}, k^i) \end{cases},$$

Now we introduce the velocity field $\mathcal{V}(y,t;\epsilon) := \Psi_t(y,t,\epsilon)$;

$$\mathcal{V}(y,t;\epsilon) = \begin{cases} \dot{k}_i(t,\epsilon) + \frac{\dot{a}_i(t,\epsilon)-\dot{k}_i(t,\epsilon)}{a^i-k^i}(y-k^i) & x \in (k^i, a^i) \\ \\ \dot{a}_{i-1}(t,\epsilon) + \frac{\dot{k}_i(t,\epsilon)-\dot{a}_{i-1}(t,\epsilon)}{k^i-a_{i-1}}(y-a_{i-1}) & x \in (a_{i-1}, k^i) \end{cases},$$

and the piecewise constant (in y) stretch function $\mathcal{S}(y,t;\epsilon)$:

$$\mathcal{S}(y,t;\epsilon) := \frac{1}{\frac{\partial \Psi}{\partial y}} = \begin{cases} \frac{a^i-k^i}{a_i(t,\epsilon)-k_i(t,\epsilon)} & y \in (k^i, a^i) \\ \\ \frac{k^i-a_{i-1}}{k_i(t,\epsilon)-a_{i-1}(t,\epsilon)} & y \in (k^i, a_{i-1}) \end{cases},$$

The outer equation (2.2) then takes the form

$$q_t - \mathcal{V} q_y - \mathcal{S} q q_y = \mathcal{S}^2 \left[\hat{W}'(q) - \epsilon^2 \mathcal{S}^2 q_{yy}\right]_{yy} \tag{A.3}$$

on each open interval (k^i, a^i) and (a^i, k^{i+1}).

Asymptotic match to $O(1)$:
Setting $\epsilon = 0$ we deduce from (A.1) that the inner solution has the form

$$\mathcal{Q}_0(X) := \tanh X \tag{A.4}$$

about the kink $k(t;\epsilon)$, and similarly, accross the anti-kink $a(t;\epsilon)$ we deduce

$$\mathcal{Q}_0(X) := -\tanh X. \tag{A.5}$$

We now match the leading order inner solutions (A.4) and (A.5) to the outer solution. Taking first an kink/anti-kink interval (k^i, a^i) and matching to order $O(1)$ we deduce, from (A.3), (A.4), and (A.5), the following boundary-value problem

$$(q_0)_t - \frac{a_0^i(t) - k_0^i(t)}{a^i - k^i} q_0 (q_0)_y = \left(\frac{a_0^i(t) - k_0^i(t)}{a^i - k^i}\right)^2 \left[(q_0)^3 - q_0\right]_{yy}$$
$$q_0\left[k^i, t\right] = 1 = q_0\left[a^i, t\right],$$

from which we conclude

$$q_0(y,t) \equiv 1 \quad \text{for} \quad y \in (k^i, a^i). \tag{A.6}$$

We deduce in a similar manner that

$$q_0(y,t) \equiv -1 \quad \text{for} \quad y \in (a^i, k^{i+1}). \tag{A.7}$$

Noting (A.2), (A.6), and (A.7), it follows from the Rankine-Hugoniot relation (R) that

$$\dot{k}_0^i(t) = 0 \qquad \text{and} \qquad \dot{a}_0^i(t) = 0. \tag{A.8}$$

Asymptotic match to $O(\epsilon)$:
From (A.8) we see that the kink and anti-kink velocities are of order $O(\epsilon)$ and therefore (A.1) is asymptotically equivalent through order $O(\epsilon)$ with the time-independent equation

$$-\epsilon Q Q_X = \left(Q^3 - Q - Q_{XX}\right)_{XX}. \tag{A.9}$$

Now (3.2) has two exact solutions $\mathcal{K}(X)$ and $\mathcal{A}(X)$ given by

$$\mathcal{K}(X) := \left(1 + \frac{\epsilon}{\sqrt{2}}\right)^{1/2} \tanh\left[\left(1 + \frac{\epsilon}{\sqrt{2}}\right)^{1/2} X\right] \qquad \text{(Kink)}$$

and

$$\mathcal{A}(X) := -\left(1 - \frac{\epsilon}{\sqrt{2}}\right)^{1/2} \tanh\left[\left(1 - \frac{\epsilon}{\sqrt{2}}\right)^{1/2} X\right], \qquad \text{(Anti-Kink)}$$

which will be matched to the outer solution. We note here that the asymptotic values as $X \to \infty$ of $\mathcal{K}(X)$ and $\mathcal{A}(X)$ are

$$\lim_{X \to \pm\infty} \mathcal{K}(X) = \pm\left(1 + \frac{\epsilon}{\sqrt{2}}\right)^{1/2}, \tag{A.10}$$

$$\lim_{X \to \pm\infty} \mathcal{A}(X) = \mp\left(1 - \frac{\epsilon}{\sqrt{2}}\right)^{1/2}. \tag{A.11}$$

Returning to (A.3), we note that $\mathcal{S} = 1 + 0(\epsilon)$ since $\dot{k}(t;\epsilon) = 0(\epsilon) = \dot{a}(t;\epsilon)$. So, it follows from (A.3), (A.6), (A.7) and the $0(\epsilon)$ matching with (A.10) and (A.11) that q_1 satisfies the following boundary value problem:

$$(q_1)_t - (q_1)_y = [2q_1]_{yy}$$
$$q_1\left(k^i, t\right) = \frac{1}{2\sqrt{2}}, \quad \text{for} \quad q_1\left(a^i, t\right) = -\frac{1}{2\sqrt{2}}.$$

Also, proceeding in a similar manner for the anti-kink/kink interval (a^i, k^{i+1}), we arrive at the companion boundary value problem

$$(q_1)_t + (q_1)_x = [2q_1]_{xx}$$
$$q_1(a^i, t) = \frac{1}{2\sqrt{2}}, \quad \text{for} \quad q_1(k^{i+1}, t) = -\frac{1}{2\sqrt{2}}$$

We conclude that

$$q_1(y,t) = q_1(y) := \begin{cases} \frac{1}{2\sqrt{2}} + \frac{1}{\sqrt{2}} \frac{1 - e^{\left[y - a^i - (k^{i+1} - a^i)\right]}}{1 - e^{-(k^{i+1} - a^i)}} & a^i \le y \le k^{i+1} \\ \frac{1}{2\sqrt{2}} - \frac{\varepsilon}{\sqrt{2}} \frac{1 - e^{-[y - k^i]}}{1 - e^{-(a^i - k^i)}} & k^i \le y \le a^i. \end{cases} \tag{A.12}$$

Hence, it follows from the Rankine-Hugoniot $\mathcal{R}$, (A.2) and (A.12) that

$$\dot{k}^i{}_1(t) = \frac{1}{4\sqrt{2}}\left[\hat{f}\left(a^i - k^i\right) - \hat{f}\left(k^i - a^{i-1}\right)\right] \tag{A.13}$$

$$\dot{a}^i{}_1(t) = \frac{1}{4\sqrt{2}}\left[\hat{f}\left(a^i - k^i\right) - \hat{f}\left(k^{i+1} - a^i\right)\right], \tag{A.14}$$

where

$$\hat{f}(l) := \frac{1}{e^l - 1}.$$

References

[1] J. W. Cahn,J. E. Hilliard, *Free energy of nonuniform systems. I. Interfacial free energy*, J. Chem. Phys. bf 28, pp 258 (1958)

[2] A. Novick-Cohen, *The Cahn-Hilliard equation: mathematical and modelling perspectives*, Adv. Math. Sci. Appl. **8**, no. 2, pp 965–985 (1998)

[3] N. Alikakos, P. Bates, G. Fusco, *Slow motion for the Cahn-Hilliard equation in one space dimension*, J. Diff. Eq. **90** 1, 81-135 (1991).

[4] A. J. Bray, *Theory of phase ordering kinetics*, Advances in Physics, **43** 3, pp357-459 (1997)

[5] J. W. Cahn, D. W. Hoffman, *A vector thermodynamics for anisotropic surfaces - II. Curved and facetted surfaces*, Acta. Metall. **22** 1205 1974

[6] J. Stewart, N. Goldenfeld, *Spinodal decomposition of a crystal surface*, Phys. Rev. A **46** 6505 (1992).

[7] A. A. Chernov, *Stability of faceted faces*, J. Cryst. Growth **24/25** 11 (1974).

[8] F. Liu, H. Metiu, *Dynamics of phase-seperation of crystal surfaces*, Phy. Rev. B **48** 5808 (1993).

[9] M. E. Gurtin, Thermomechanics of Evolving Phase Boundaries in the Plane, Clarendon Press, Oxford, 1993

[10] A. A. Golovin, S. H. Davis, A. A. Nepomnyashchy, *A convective Cahn-Hilliard model for the formation of facets and corners in crystal growth*, Physica D **118** (1998), pp 202-230.

[11] K. Leung, *Theory of morphological instability in driven systems*, J. Stat. Phys. **61** (1990), 345.

[12] A. A. Golovin, A. A. Nepomnyashchy, S. H. Davis, M. A. Zaks, *Convective Cahn-Hilliard models: from coarsening to roughening*, Phys. Rev. Lett. **86** 8 (2001) pp. 1550-1553.

[13] C. L. Emmott, A. J. Bray, *Coarsening dynamics of a one-dimensional driven Cahn-Hilliard system*, Phys. Rev. E **54** (1996) 4568.

[14] P. Smilauer, M Rost, J. Krug, *Fast coarsening in unstable epitaxy with desorption*, Phys. Rev. E **59** 6 (1999) 6263

[15] S. J. Watson *Crystal growth, coarsening and the convective Cahn-Hilliard equation*, in preparation.

[16] S. J. Watson,, *The spectrum and generalized eigenvector basis of alternating circulant matrices*, submitted to Linear Algebra and its Applications (2002).